Supporting Information

Zhao et al. 10.1073/pnas.1300968110

SI Methods

Animal Care Ethics. All zebrafish experiments were conducted according to Yale Animal Resources Center and Institutional Animal Care and Use Committee guidelines.

Zebrafish Husbandry. Zebrafish were maintained following standard protocols (1). Embryos were obtained through natural spawning.

Histological Analysis. Embryos were fixed in Bouin's fixative (Fisher Scientific) overnight at room temperature, and embedded with a JB-4 kit (Polysciences). Blocks were cut into 4-μm sections and stained with hematoxylin and eosin.

Molecular Cloning. Full-length *reptin* coding sequence was amplified from a zebrafish cDNA pool by PCR and cloned into a Gateway entry vector. *Reptin* tagged with EGFP or Flag was generated using the Gateway cloning kit following a previously described strategy (2). Deletion and mutant constructs of *seahorse* and *reptin* were generated via PCR cloning.

Microinjection. Microinjection was performed as described previously (3). mRNA was transcribed in vitro using the mMESSAGE mMACHINE kit (Ambion). Morpholino oligonucleotides (MOs) were synthesized by Gene Tools (Philomath). All mRNAs or morpholinos were injected into embryos at the one- to two-cell stage. For morpholinos, 5′-TTGCCACCTGCGCTGCCATGTTTTC-3′ was used to block the translation of *reptin*. 5′-GACTCAGGGCAGTTATAAGAACGTA-3′ was used to block the translation of *ift172* (4). 5′-GCGGACCATGACTTGCTGGTCTAGT-3′ was used to block the translation of *seahorse* (5). A standard morpholino oligo (5′-CCTCTTACCTCAGTTACAATTTATA-3′) was used as a negative control.

For the synergistic assay between *reptin* and *ift172*, 20 pg *reptin* MO and 240 pg *ift172* MO were coinjected in the double morpholino group, whereas the control groups were coinjected with either 20 pg *reptin* MO and 240 pg control MO or 240 pg *ift172* MO and 20 pg control MO. For the synergistic assay between *reptin* and *seahorse*, 20 pg *reptin* MO and 100 pg *seahorse* MO were coinjected in the double morpholino group, whereas the control groups were coinjected with either 20 pg *reptin* MO and 100 pg control MO or 100 pg *seahose* MO and 20 pg control MO.

Immunohistochemistry. Zebrafish embryos were fixed in Dent's fixative and immunostainning was performed as before (6, 7). Slides were mounted using Vectashield Hard Set mounting medium (Vector) and analyzed with a Nikon Eclipse E800 microscope.

RT-PCR. Total RNA was extracted from zebrafish embryos with TRIzol reagent (Invitrogen) following manufacturer's instructions. First-stand cDNA was synthesized with SuperScript II reverse transcriptase (Invitrogen) and subsequently amplified by PCR.

Whole-Mount in Situ Hybridization. Whole-mount in situ hybridization was performed as before (8, 9). Briefly, embryos were fixed in 1:4 freshly diluted formalin in PBS with 0.1% Tween-20 (PBT) and incubated with digoxigenin-UTP labeled probes. Alkaline phosphatase-coupled anti-digoxigenin antibody (Roche, 1:1,000 dilution) was used to localize hybridized probes and NBT (Nitro Blue Tetrazolium)/BCIP (5-Bromo-4-Chloro-3-Indolyl-Phosphate) (Roche) was used as the chromogenic substrate to produce blue precipitates.

Protein Extraction, Immunoprecipitation, and Western Blotting. For total lysate, embryos were deyolked and homogenized in SDS sample buffer, boiled for 5 min, and cleared by centrifugation at top speed for 5 min. For immunoprecipitation (IP), embryo lysates were prepared in TG buffer (PBS with 0.1% Triton X-100, 1% glycerol). Lysates were then incubated with respective antibodies followed by protein A beads (Pierce) at 4 °C. Horseradish peroxidase-conjugated secondary antibodies (Jackson ImmunoResearch) were used at 1:5,000. Membranes were subjected to enhanced chemiluminescence detection using the Western Lighting kit (Perkin-Elmer Life Sciences).

High-Speed Videomicroscopy of Cilia. Mounting and imaging of cilia in live zebrafish embryos were performed following a previously published protocol (10). To avoid perturbing cilia motility, no anesthetics or immobilizing reagents were used. Videomicroscopy was performed using an inverted Axiovert 200m (Zeiss) microscope with a 63× C-Apochromat water objective and a MotionPro Y4-Lite (Integrated Design Tools) high-speed camera. All acquisitions were collected at a rate of 2,000 frames per second with a 499-μs exposure time and a 1,016 × 1,016 pixel resolution using Motion Studio (Integrated Design Tools). Cilia beating dynamics were analyzed using kymograph in MetaMorph (Molecular Devices). Movie clips were prepared using iMovie (Apple) and Premiere Pro (Adobe).

Electron Microscopy. Zebrafish embryos were fixed in Karnoysky fixative for 1 h at 4 °C, washed with cacodylate buffer, postfixed in Palade's osmium for 1 h at 4 °C, washed with cacodylate buffer, stained with Kellenberger for 1 h at room temperature, and dehydrated in ethanol. Embryos were subsequently infiltrated through a propylene oxide/Epon series, embedded in Epon, and sectioned. Sections were poststained with uranyl acetate and lead citrate and examined with a Zeiss EM910 electron microscope.

Yeast Two-Hybrid. Yeast two-hybrid assay was conducted using the MATCHMAKER GAL4 Two-Hybrid System (Clontech). Plasmids in pGBKT7 and pGADT7 backbones were transformed into AH109 using a lithium acetate-mediated method following manufacturer's instructions.

Quantitative PCR. Total RNA was extracted from 2-d postfertilization (dpf) embryos using a Direct-zol RNA miniprep kit (Zymo Research), following manufacturer's instructions. First-strand cDNA was then synthesized using SuperScript II reverse transcriptase (Invitrogen). All quantitative PCR (qPCR) reactions were performed using the KAPA SYBR Fast Bio-Rad iCycler 2× qPCR master mix (KAPA biosystems) on a C1000 Thermal Cycler (Bio-Rad) following manufacturer's instructions. Primers were designed using the National Center for Biotechnology Information Primer-Blast software with each primer pair spanning at least one exon–exon junction.

Tail Biopsies and Genotyping. Tail biopsies were performed by cutting 1–2 mm tissue from the tail tip of 2-mo-old fish anesthetized in Tricaine (Sigma). Tail tissues were incubated in 50 μL SDS lysis buffer (100 mM Tris pH 8.3, 200 mM NaCl, 0.4% SDS, 5 mM EDTA) with freshly added proteinase K (final concentration: 200 μg/mL) at 55 °C on a rocker table for 2 h to overnight. The concentrated tail DNA was then diluted 20-fold in water and incubated at 94 °C for 15 min to inactivate pro-

teinase K. One microliter of the diluted tail DNA was used to set up a 20-μL PCR for genotyping.

The double homozygotes *hi2394; hi2211* and *hi2394; hi3308* were generated as previously described (5). Embryos were numbered and imaged at 3 dpf and then lysed in SDS lysis buffer in individual tubes. Genotyping was performed using three primers for each locus: two for genomic sequences flanking the proviral insertion and one in the proviral insertion. In the absence of the proviral insertion, amplification would occur between the genomic pair. In contrast, in the presence of the 10-kb proviral insertion, amplification would only occur between the proviral-specific primer and one of the genomic pair. The genotype of each offspring was recorded and matched with its images.

Statistical Analysis. For the rescue experiment and the synergistic assays, three independent experiments were performed to examine the body curvature and kidney cyst phenotypes. A Cochran-Mantel-Haenszel test was conducted using the R program (11). For motility and dynein arm numbers, Student *t* tests (two-tail, equal variance) were performed using Microsoft Excel.

***In Silico* Analysis of Protein Domain Prediction.** SMART (http://smart.embl-heidelberg.de) was used to identify the presence of the AAA domain in Reptin. cNLS mapper (http://nls-mapper.iab.keio.ac.jp) was used to identify the nuclear localization signal. Protein alignment of Seahorse protein fragment was completed by Lasergene MegAlign (DNASTAR).

Antibodies and Fluorescent Dyes. Chicken anti-cdh17 is a custom antibody produced by Covance. A region corresponding to amino acids 639–819 of Cdh17 was produced as GST fusion protein in *Escherichia coli* and purified following the manufacturer's protocol with the pGEX system (GE Healthcare LifeSciences) and used as the antigen. IgG was purified from serum with CM Affi-Gel blue gel following manufacturer's instruction manual (Bio-Rad). Anti-Cdh17 was used at 1:500 dilution. Custom rabbit polyclonal anti-Seahorse has been described before (5); 1:1,000 was used in immunostaining and Western blotting.

The following commercial antibodies were used: rabbit polyclonal anti-Reptin antibody (Abcam; ab91462, 1:1,000 in immunostaining and Western blotting); mouse monoclonal anti-acetylated tubulin antibody (Sigma-Aldrich; clone 6–11B-1, 1:5,000 in immunostaining); rabbit polyclonal anti-γH2AX antibody (courtesy of James Amatruda, University of Texas Southwestern, Dallas, 1:1,000 in immunostaining); goat anti-eGFP antibody (Rockland Immunochemicals; 600–132-215, 1:500 in immunostaining); mouse monoclonal anti–β-tubulin antibody (Sigma; T4026, 1:8,000 in Western blotting); mouse monoclonal anti-Flag M2 antibody (Sigma; clone M2, 1:500 in Western blotting); and mouse anti-GFP IgG (Roche; clone 7.1 and 13.1, 1:1,000 in Western blotting).

Two fluorescence dyes: DAPI (Invitrogen; D3571, 1:1,000) and rhodamine phalloidin (Invitrogen; R415, 1:1,000) were used to stain DNA and F-actin, respectively. Formalin-fixed embryos were used for phallodin staining.

Primers. Primers used for genotyping are listed below:

Hi2394 (viral): 5′-CTGTTCCATCTGTTCCTGAC-3′
Hi2394 (genomic_1): 5′-ACATGGCAGCGCAGGTATGT-3′
Hi2394 (genomic_2): 5′-CGCTTGCGTTGCCATAGTG-3′
Hi3308 (viral): 5′-AGTCCTCCGATTGACTGAGT-3′
Hi3308 (genomic_1): 5′-CACAAGTGGTGCAGAGACCTC-3′
Hi3308 (genomic_2): 5′-CCAATCTATTTTTGACCCAGTTACAC-3′
Hi2211 (viral): 5′-CTGTTCCATCTGTTCCTGAC-3′
Hi2211 (genomic_2): 5′-GCCATAGACTTGACCACATAGG-3′

Primers used in qPCR are listed below:

ef1α (housekeeping gene): forward: 5′-GGAGGCCAGCTCAAACATGGGC-3′
reverse: 5′-AGGGCATCAAGAAGAGTAGTACCGC-3′
foxj1a: forward: 5′-AGATCCCACCTGGCAGAACT-3′
reverse: 5′-TTGCCCGGTTCATCCTTCTG-3′
dnah9: forward: 5′-TACTGGTGGACAAGGTTGTGG-3′
reverse: 5′-ACACGTTGTTTTGAAGGGCG-3′
dnai1: Forward: 5′-AATGTCTGAGGAGAAACAGCCG-3′
Reverse: 5′-ACTGGTTGCTGCATTTAGTCG-3′
dnal1: forward: 5′-AATGGACTCGAGGCAGTGGG-3′
reverse: 5′-GCCTCCTCTATCCAGTTGCC-3′
lrrc50(Dnaaf1): forward: 5′-CATCACAGAGTGGGATGCGT-3′
reverse: 5′-GAGATTGGTCAAGGGCCACA-3′
ktu(Dnaaf2): forward: 5′-GGTCCTGACCCACCAATGAT-3′
reverse: 5′-CTGATGACATTAGAAGAGGAGAGCA-3′
pf22(Dnaaf3): forward: 5′-CATCAGAGAGGATGTGGCGTCAT-3′
reverse: 5′-GAAGACTCGAGTTGAAAGCAGACTC-3′

1. Westerfield M (2000) *The Zebrafish Book. A Guide for the Laboratory Use of Zebrafish (Danio rerio)* (Univ Oregon Press, Eugene, OR).
2. Kwan KM, et al. (2007) The Tol2kit: A multisite gateway-based construction kit for Tol2 transposon transgenesis constructs. *Dev Dyn* 236(11):3088–3099.
3. Yuan S, Sun Z (2009) Microinjection of mRNA and morpholino antisense oligonucleotides in zebrafish embryos. *J Vis Exp* (27):1113.
4. Cao Y, Park A, Sun Z (2010) Intraflagellar transport proteins are essential for cilia formation and for planar cell polarity. *J Am Soc Nephrol* 21(8):1326–1333.
5. Kishimoto N, Cao Y, Park A, Sun Z (2008) Cystic kidney gene seahorse regulates cilia-mediated processes and Wnt pathways. *Dev Cell* 14(6):954–961.
6. Drummond IA, et al. (1998) Early development of the zebrafish pronephros and analysis of mutations affecting pronephric function. *Development* 125(23):4655–4667.
7. Dent JA, Polson AG, Klymkowsky MW (1989) A whole-mount immunocytochemical analysis of the expression of the intermediate filament protein vimentin in Xenopus. *Development* 105(1):61–74.
8. Duldulao NA, Lee S, Sun Z (2009) Cilia localization is essential for in vivo functions of the Joubert syndrome protein Arl13b/Scorpion. *Development* 136(23):4033–4042.
9. Hauptmann G, Gerster T (2000) Multicolor whole-mount in situ hybridization. *Methods Mol Biol* 137:139–148.
10. Yuan S, et al. (2012) Target-of-rapamycin complex 1 (Torc1) signaling modulates cilia size and function through protein synthesis regulation. *Proc Natl Acad Sci USA* 109(6):2021–2026.
11. R Development Core Team (2012) R: A language and environment for statistical computing (R Foundation for Statistical Computing, Vienna).

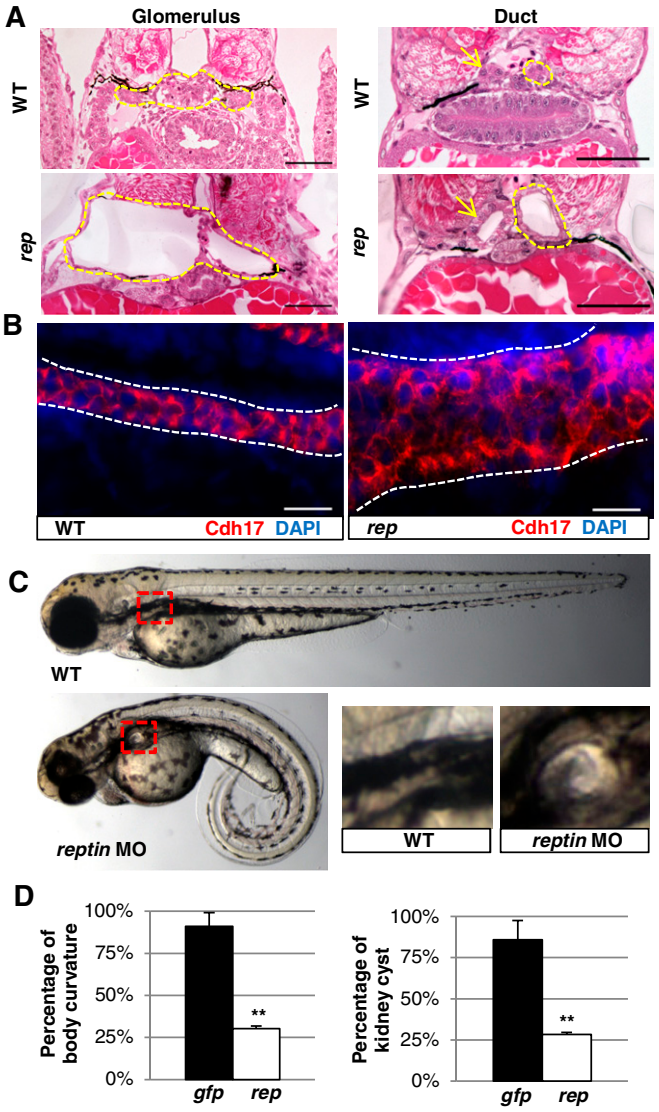

Fig. S1. *Reptin*^{hi2394} mutants and *reptin* morphants display cilia-associated phenotypes. (*A*) Cross-sections of the glomerular–tubular region and the posterior pronephric duct region of a *reptin*^{hi2394} mutant (*rep*) and a wild-type sibling (WT) at 5 dpf. Yellow dotted lines show the border of the glomerular–tubular region on the *Left* and the duct on the *Right*; yellow arrows point to the duct on the *Left*. (Scale bar, 50 μm.) (*B*) Whole-mount immunostaining with anti-Cdh17 (Cdh17, red) showing increased diameter of the pronephric duct (bordered by white line) in a side view of a *reptin*^{hi2394} mutant (*rep*) compared with a wild-type embryo (WT) at 4 dpf. (Scale bar, 20 μm.) (*C*) *Reptin* morphant (*rep* MO) at 3 dpf displaying kidney cyst (red box) and body curvature, compared with a control MO injected embryo (WT). The kidney regions are magnified at *Lower Right*. (*D*) Wild-type embryos coinjected with *reptin* MOs and *reptin* (with 5 mismathed nucleotides) mRNA (*rep*) showing reduced percentages of body curvature (*Left*) and kidney cyst (*Right*), compared with the *reptin* MOs and *eGFP* mRNA coinjection group (*gfp*). Data are represented as mean + SD from three replicates. $^{**}P < 0.01$.

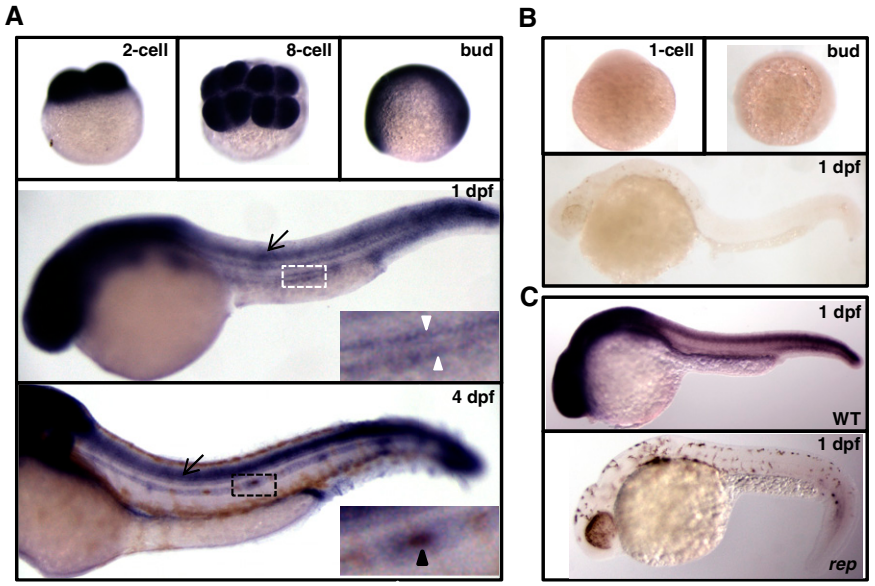

Fig. S2. The distribution pattern of *reptin* transcripts during zebrafish development. (*A*) In situ hybridization (ISH) for *reptin* on wild-type embryos fixed at different stages. Black arrows point to the neural tube. *Insets* are enlarged images showing the bilateral pronerphric ducts pointed out by white arrowheads (boxed by white dotted line in the *Middle*) and the lateral line organ pointed out by a black arrowhead (boxed by black dotted line at *Bottom*). (*B*) Sense control for *A*. (*C*) ISH for *reptin* on a 1-dpf *reptin*^{hi2394} mutant (*rep*, *Lower*) and a wild-type sibling (WT, *Upper*).

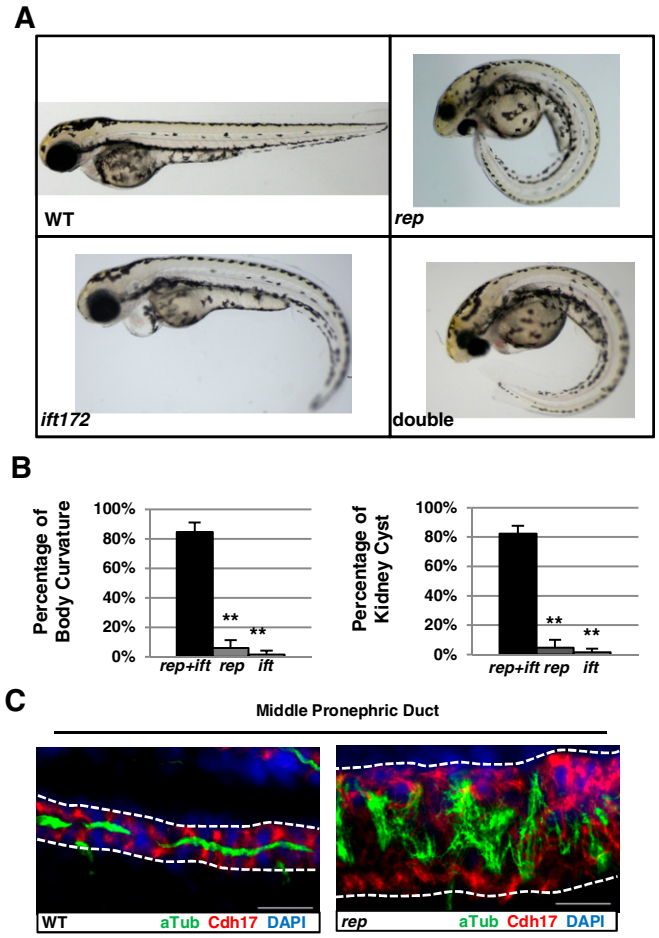

Fig. S3. *Reptin* genetically interacts with the cilia biogenesis gene *ift172*, but is dispensable for cilia biogenesis. (*A*) Phenotypes of *reptin*^{hi2394}; *ift172*^{hi2211} double mutants (double) and single mutants of either genes at 4 dpf. WT, wild-type sibling. (*B*) Percentage of embryos showing body curvature (*Left*) and kidney cysts (*Right*). A total of 82.2% embryos show kidney cyst formation and 84.6% embryos show body curvature in the *reptin* MO and *ift172* MO co-injection group (*rep+ift)*, compared with 4.7% cyst formation and 5.9% body curvature in the *reptin* MO and control MO coinjection group (*rep*) or 1.5% cyst formation and body curvature in the *ift172* MO and control MO coinjection group (*ift)*. Data are represented as mean + SD from three replicates. $^{**}P < 0.01$. (*C*) Immunostaining showing cilia (stained with antiacetylated tubulin in green) in *reptin*^{hi2394} mutants in the middle region of the pronephric duct (stained with anti-Cdh17, in red, lined with dotted lines). WT, wild type; *rep*, *reptin*^{hi2394}. (Scale bar, 20 μm.)

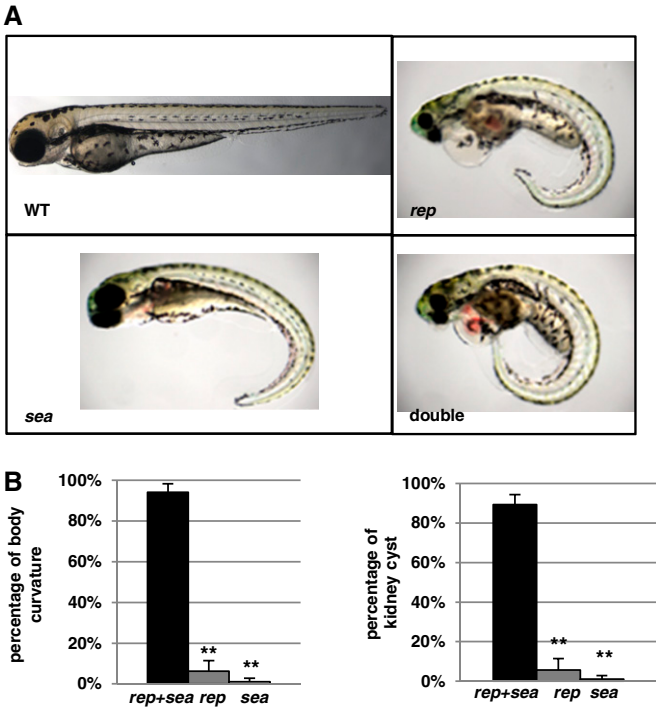

Fig. S4. *Reptin* genetically interact with *seahorse/lrrc6*. (*A*) *Reptin*^{hi2394}; *seahorse*^{hi3308} double mutants (double) show similar cystic kidney phenotype as single mutants of either gene at 4 dpf. (*B*) Percentage of embryos showing body curvature (*Left*) and kidney cysts (*Right*). A total of 89.3% embryos show kidney cyst formation and 94.1% embryos show body curvature in the *reptin* MO and *seahorse* MO coinjection group (*rep+sea*), compared with 1% cyst formation and body curvature in the *seahorse* MO and control MO coinjection group (*sea*) or 5.7% cyst formation and 6.2% body curvature in the *reptin* MO and control MO coinjection group (*rep*). Data are represented as mean + SD from three replicates. $^{**}P < 0.01$.

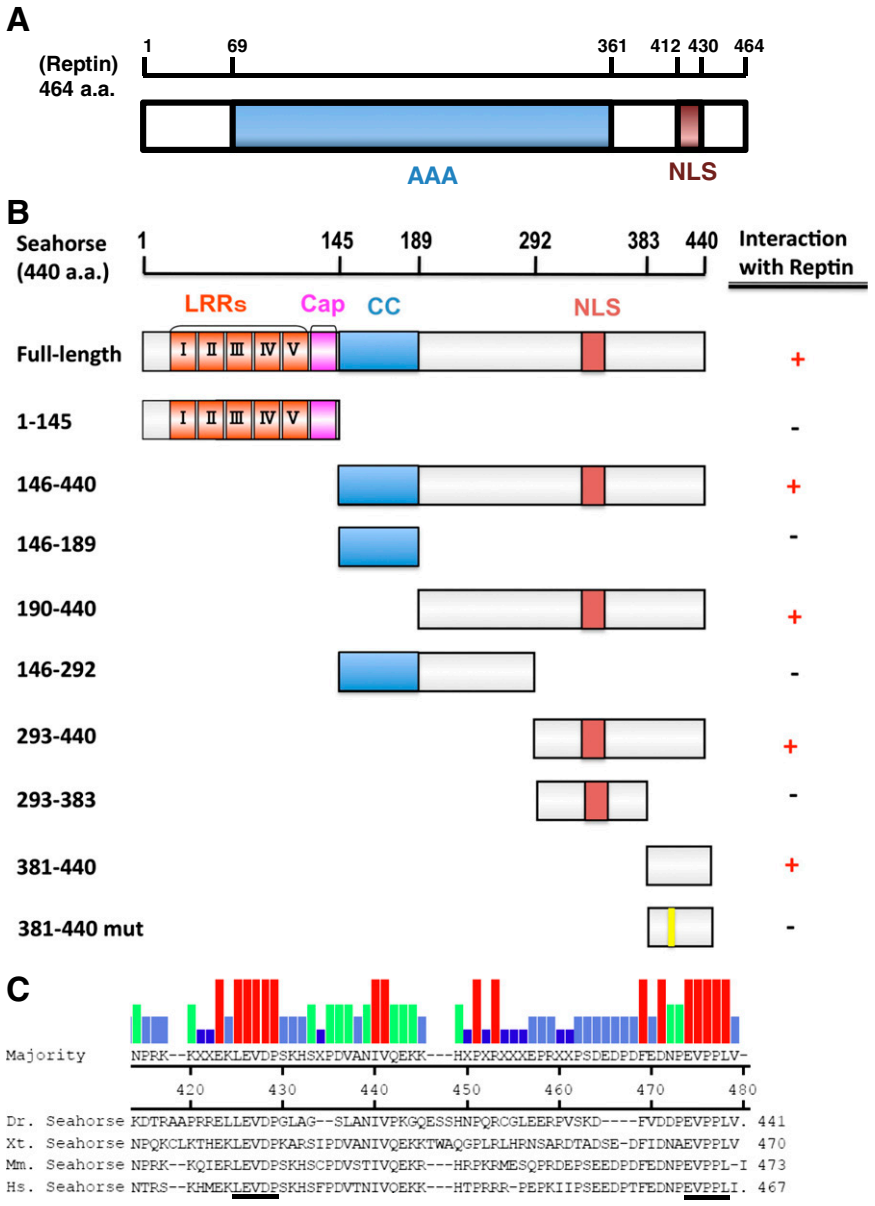

Fig. S5. Structures of Reptin and Seahorse. (*A*) Protein domain prediction of Reptin showing an AAA domain at amino acids 69–361 and a nuclear localization signal (NLS) at amino acids 412–430. (*B*) Serial deletion analysis of the Reptin-interacting domain in Seahorse, which contains leucine-rich repeats (LRRs), a LLR cap, a coiled-coil region (CC), and a nuclear localization signal (NLS). 381–440 mut, amino acids 381–440 with amino acids 392–396 substituted with alanines. (*C*) Protein sequence alignment of the minimal Reptin-interacting region in Lrrc6/Seahorse (amino acids 381–440) among zebrafish (*Danio rerio*), frog (*Xenopus tropicalis*), mouse (*Mus musculus*), and human (*Homo sapiens*). The two conserved regions (amino acids 392–396 and 435–439) are underlined.

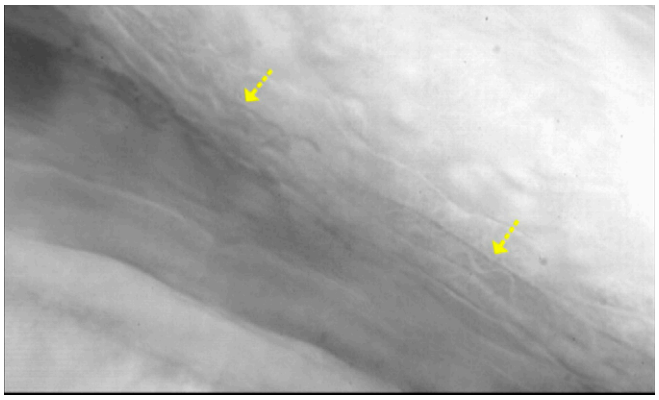

Movie S1. Paralyzed cilia in the pronephric duct of a *reptin*^{hi2394} mutant. Beating cilia bundles are shown in the lumen of the posterior pronephric duct in a wild-type sibling and paralyzed cilia in a *reptin*^{hi2394} mutant at 3 dpf. Yellow arrows point to examples of beating or paralyzed cilia.

Movie S1

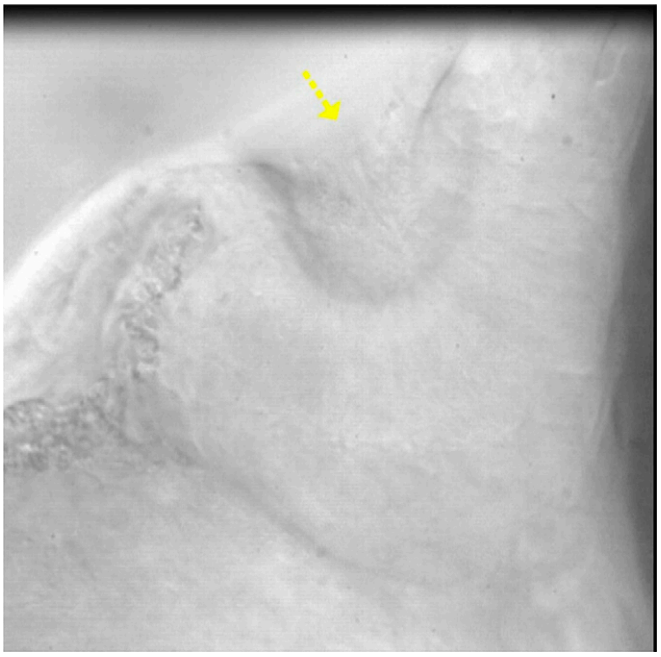

Movie S2. Paralyzed cilia in the olfactory placode of a *reptin*^{hi2394} mutant. Beating cilia are shown on the border of an olfactory placode in a wild-type sibling and completely paralyzed cilia in a *reptin*^{hi2394} mutant at 3 dpf. Yellow arrows point to beating cilia or paralyzed cilia.

Movie S2

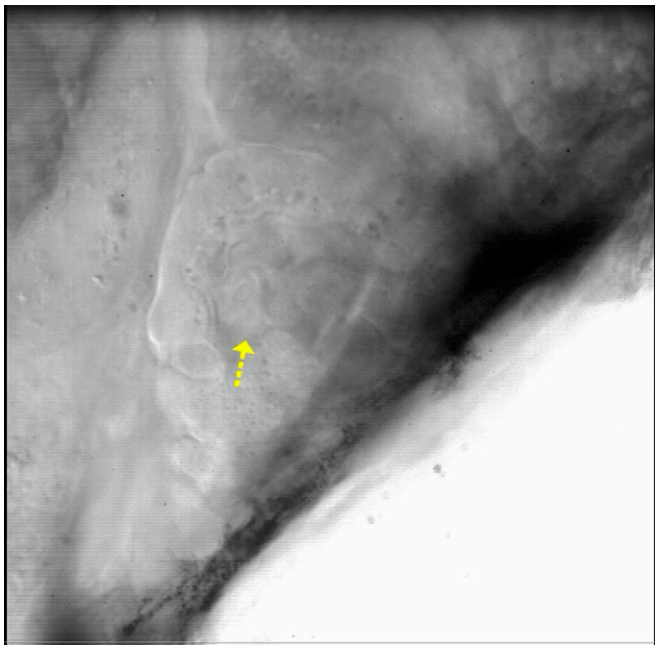

Movie S3. Cilia motility defect in the anterior pronephric duct of a *seahorse*^{hi3308} mutant. Beating cilia are shown in the lumen of the anterior pronephric duct in a wild-type sibling and variable cilia beating in a *seahorse*^{hi3308} mutant at 3 dpf. Yellow arrows point to cilia.

Movie S3

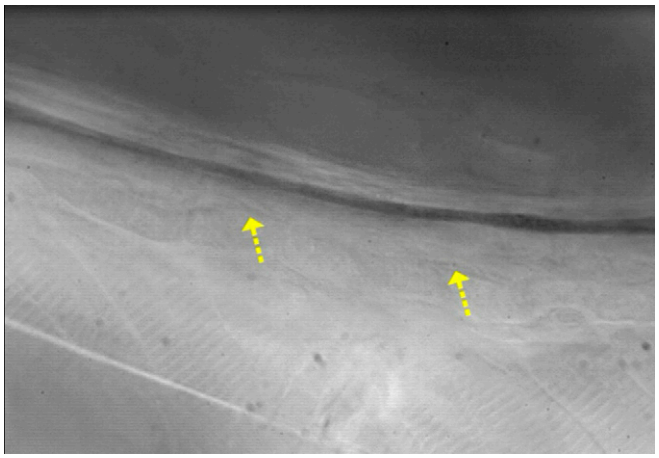

Movie S4. Cilia motility defect in the posterior pronephric duct of a *seahorse*^{hi3308} mutant. Beating cilia bundles are shown in the lumen of the posterior pronephric duct in a wild-type sibling and a *seahorse*^{hi3308} mutant. Yellow arrows point to beating cilia. Note the slower beating frequency in the mutant.

Movie S4

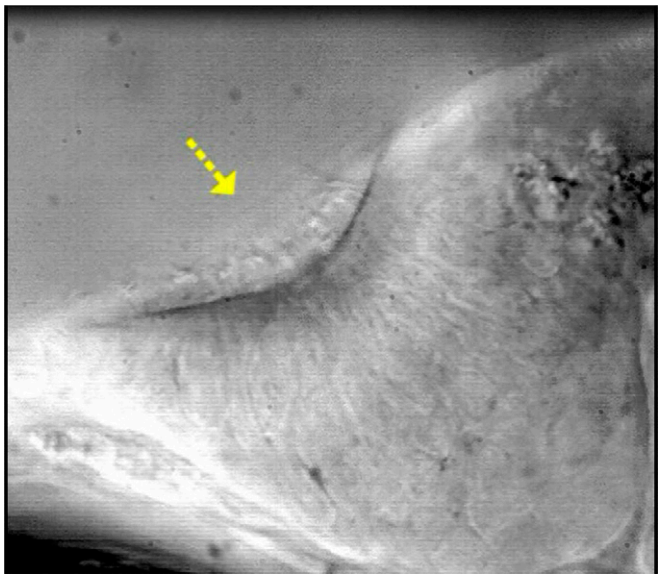

Movie S5. Cilia motility defect in the olfactory placode of a *seahorse*^{hi3308} mutant. Beating cilia are shown at the border of the olfactory placode of a wild-type sibling and variable cilia beating in a *seahorse*^{hi3308} mutant at 3 dpf. Yellow arrows point to beating or paralyzed cilia.

Movie S5